UC San Diego
UC San Diego Previously Published Works

Title
Stretchable Textile Bands for Ambulatory Electrocardiogram and Oximetry

Permalink
https://escholarship.org/uc/item/5wd460cq

Journal
IEEE Journal on Flexible Electronics, 1(4)

ISSN
2768-167X

Authors
Liu, Jiaxi
Le, Thy
Sadatian, Ellie
et al.

Publication Date
2022-10-01

DOI
10.1109/jflex.2022.3220138

Peer reviewed

Stretchable Textile Bands for Ambulatory Electrocardiogram and Oximetry

Jiaxi Liu,[1] Thy Le,[1] Ellie Sadatian,[1] Lulu Yao,[2] Harinath Garudadri,[3] Stephen Dunphy,[4] Christian McClung,[4] and Tse Nga Ng[1*]

[1] Department of Electrical and Computer Engineering, University of California San Diego, La Jolla, CA 92093, U.S.A.

[2] Materials Science Engineering Program, University of California San Diego, La Jolla, CA 92093, U.S.A.

[3] Qualcomm Institute, University of California San Diego, La Jolla, CA 92093, U.S.A.

[4] CBooth Innovations, P.O. Box 5010 PMB 079, Rancho Santa Fe, CA 92067, U.S.A.

*Corresponding email: tnn046@ucsd.edu

Abstract—**This work presents a vital sign monitoring interface combining electrocardiogram (ECG) and reflective photoplethysmography (PPG) acquisition on stretchable kinesiology tapes. The integrated textile bands are less prone to electrode misplacement and deliver high-quality diagnostic ECG signals with dry electrodes. The reflective PPG measured over the subclavian artery is used to track blood oxygen saturation, and in combination with ECG, enables the determination of pulse transit time and inference of blood pressure. This multimodal interface improves clinical work flows because it is easy to don, reduce motion artifacts, and facilitate more efficient and accurate diagnosis in emergency settings.**

Index Terms—**electrocardiogram, pulse oximetry, blood pressure, stretchable electronics**

I. INTRODUCTION

In emergency care, medical professionals need to know a patient's vital signs to give appropriate treatments for the best outcome. The standard vital signs includes heart rate, blood pressure, respiratory rate, and temperature. For any patient with chest pain, it is recommended that a 12-lead electrocardiogram (ECG) be recorded within 10 minutes upon arrival in the emergency room to enable timely diagnosis of acute heart disease and decrease mortality.[1] However, it has been challenging to carry out the clinical standard 12-lead ECG correctly in emergency settings. According to Medani *et al*., only 34% of the precordial leads are placed correctly in a study of 100 trained technicians.[2] The poor implementation is caused by typical setups in which the ten electrodes are independent and wired up separately, often contributing to electrode placement errors or transposition of wires, and the placement process is time-consuming. To overcome the equipment limitations, a better device configuration is urgently needed to facilitate fast and correct ECG measurements.

In addition to ECG rhythms, monitoring other vital signs typically requires connecting a patient to multiple equipment, including a blood pressure cuff and a photoplethysmography (PPG) sensor tracking blood oxygenation. Applying these additional devices is time-consuming; it is very desirable to integrate the different devices into a convenient design that allows quick application and reduces inefficiency in emergency care. For this goal, we present a new interface design that integrate ECG electrodes and PPG electronics into easy-to-don textile bands, and this multimodal approach also adds the capability to infer blood pressure changes during continuous monitoring.[3]

While wearable monitors of vital signs have been demonstrated previously,[4–6] most of the prior works had decreased the number of ECG electrodes to reduce system complexity and focus mainly on identifying arrhythmias but cannot provide a full set of clinical diagnostic characteristics. In particular, the precordial leads were often dropped, yet the information from those leads are critical for diagnosing morphological changes in different parts of the heart. A recent study by Roy *et al*. has improved their ECG interface to include the 6 precordial leads on one bendable strip;[7] however, because the substrate was not stretchable, the strip would not be conformable over curvy breast tissues and lack the adjustability to precisely match electrode spacing to the patient size. It was limited to ECG and not a multimodal interface. Multimodal monitoring poses additional fabrication challenges yet is essential to gain better understandings of the patient's health status.

In this work we repurpose kinesiology tapes (KT) to serve as stretchable textile substrates[8] for our integrated ECG and PPG platform that measures three of the vital signals: heart rate, oxygenation (a proxy for respiratory rate), and blood pressure. Compared to conventional plastic substrates such as polyester or polydimethylsiloxane (PDMS) elastomer, the KT substrates are more breathable and less susceptible to delamination. On the adhesive side of the KT textile, the ECG leads are printed with stretchable conductive materials and interconnect patterns to form conformal dry electrodes with a low noise level better than commercial 3M Red Dot™ gel electrodes. Moreover, as the substrate is stretched, the distances between precordial electrodes are increased by the same ratio, which keeps the electrodes at correct locations upon expansion/contraction of the chest during breathing. The assembly of the PPG (also known as pulse oximetry) components on KT substrates results in a flexible circuit that adheres very well to the surface of skin and significantly reduce motion artifacts in the PPG measurements for tracking blood oxygenation.

Finally, the synergistic combination of ECG and PPG allows us to extract the pulse arrival time and infer changes in blood pressure. Our system can be an alternative to blood pressure cuffs; in many instances a pressure cuff placed ipsilateral to the PPG sensor introduces errors when the applied pressure occludes arterial flow and leads to unreliable measurements. Here our vital sign monitoring interface is easy to apply and minimizes placement error and is comfortable for day-long wear. The device provides an opportunity for continuous tracking of a patient's status, including during emergency defibrillation or rehabilitation activities which can be challenging measurements because of motion artifacts.
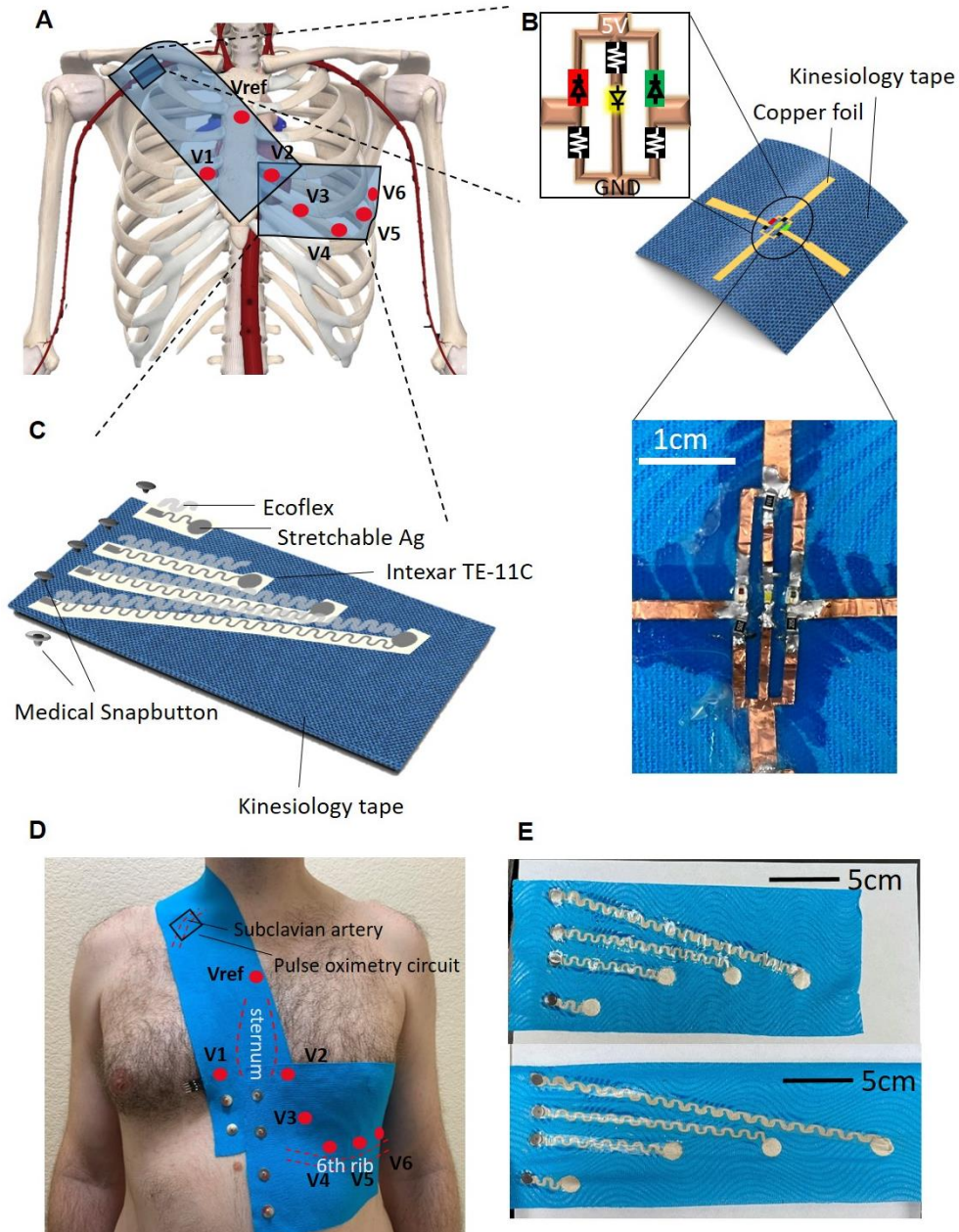
Figure 1. Illustrations and photographs of stretchable textile bands with ECG electrodes and pulse oximetry electronics. A) A schematic of device locations in relation to the human body. The pulse oximetry unit is placed over the right subclavian artery. The locations of ECG precordial leads are denoted by red dots, with V1 and V2 on the tape with the pulse oximeter and V3-V6 on another tape stretched across lower sternum to midaxillary line. The human body image is from Complete Anatomy, thanks to @3D4Medical. B) The circuit, layout schematics, and a photograph of the pulse oximetry unit. C) An exploded view of precordial leads. From bottom to top, the layers are kinesiology tape, Dupont™ INTEXAR™ TE-11C film, screen-printed. stretchable silver ink, and Ecoflex. The medical snap buttons are installed before the Ecoflex encapsulation layer. D) A photograph of the bands mounted on a person. The red dots and dashed lines are added to the photograph to indicate electrode locations and anatomical parts, respectively. The Vref electrode is used as a close approximation to the virtual Wilson Central Terminal reference. E) Photographs of the band with V3-V6 precordial leads. Top: in the original unstretched state. Bottom: the electrodes are stretched uniaxially to 130% of its original length.

II. RESULTS AND DISCUSSION

The schematics of our integrated ECG and PPG textile bands is illustrated in **Figure 1A**, indicating the device locations with respect to the human anatomy. The PPG circuit, also known as the pulse oximetry unit in **Figure 1B**, is consisted of a light source and two light detectors to monitor changes in the optical absorption of arterial vessels correlated to the oxygenation level. In our design, the PPG unit is placed over

the right subclavian artery, and the PPG unit and ECG precordial leads V1 and V2 are integrated on one KT band that extends from the left shoulder to the sternum. The precordial leads V3 to V6 are integrated on another KT band spanning across the midsternal line to the anterior axillary line on the body.

A. Stretchable ECG interface

The structure of our ECG measurement interface is shown in **Figure 1C**, and the detailed fabrication procedure is explained in the Experimental Section. The fabrication process is low-cost for the interface to be disposable. In brief, the patterns for electrodes and interconnects were screen-printed using a stretchable conductive silver ink[9] onto a base film of Dupont Intexar™ polymer, which was then heat pressed onto the KT band. The interconnects were in serpentine patterns to increase uniaxial stretchability.[10,11] Medical snap-buttons were mounted at the ends of the interconnects to serve as connectors to our readout board, and the snap-button connectors were also compatible with common bedside ECG equipment. A thin encapsulation layer of Ecoflex™ was screen-printed to cover the snap button studs and the silver traces except for the electrode area intended for contact with the patient body. Here the collection of ECG electrodes leveraged the strong yet hypoallergenic adhesive of the KT band to secure the electrodes in place as seen in **Figure 1D** without the use of hydrogel. Thus the band avoids the disadvantages of wet gel electrodes, such as the possibility of skin irritation and signal degradation due to gel dehydration.[12–14] Our dry electrode patch is non-intrusive and stable for long-term monitoring.

The impedance across an exemplar dry electrode was comparable to a commercial gel electrode (3M Red Dot™ 2560), and the measured values showed that the dry electrode offered a more conductive surface, as evident in the supplemental Figure S1 where the measurent were carried out with electrodes placed face-to-face. The metal-to-metal surface has a lower impedance than the gel-to-gel surface. In Figure S2, The noise spectral density of the dry electrode was lower than the gel electrode and would lead to improvements in the signal-to-noise ratio. The change in resistance of V3-V6 precordial leads was characterized under uniaxial stretching as shown in **Figure 1E**. While the resistance of the longest V6 lead increased by 4 times when stretched to 1.3 times of its original length (Figure S3), the highest resistance value was still only 40 Ω, significantly below the electrode-skin interfacial resistance such that this interconnect resistance change under stretching would not affect signal quality. The interconnects reached 70% tensile strain before failure due to cracking. Our measurements to 30% tensile strain are meant to accommodate chest expansions during breathing and to adjust electrode spacing for different individual sizes.

The ECG characteristics taken using the KT bands on a healthy volunteer is shown in **Figure 2A**. The precordial lead measurements were taken with respect to a reference electrode placed on top of the sternum, which has been demonstrated as a close equivalent[15] to the virtual Wilson Central Terminal (WCT) averaged from three limb leads. The sternum reference is used here when the conventional limb lead electrodes are not connected, but the reference can be easily reverted back to virtual WCT when limb leads are present.

In the set of V1 to V6 characteristics, the R peaks changed in sign and magnitude, capturing the ventricular depolarization impulse as a function of measurement locations across the chest. The signal-to-noise ratio (SNR) for each lead location is displayed in **Table 1,** in which the SNRs for the KT band electrodes were above 13.2 dB and higher than the 3M RedDot™ electrodes recording at the same locations. To measure the SNR of stretched electrodes, the KT band was stretched to the designated measurement locations and then pressed down to stick on the body. The improvement of SNR with KT bands was attributed to reduced environmental interference and motion artifacts by the elimination of dangling wires that are necessary in conventional electrode setups. This report mainly discusses measurement results from the set of precordial leads V1-V6, but the three limb electrodes have also been fabricated by the same process yielding measurement results for the limb (I, II, III) leads shown in Figure S4 in the Supplement. The same limb electrodes can be used to obtain augmented (aVR, aVL, aVF) leads measurements, and thus the KT band interface is suitable for taking the clinical standard 12-lead ECG.

Table 1. Comparison of signal-to-noise ratios of KT electrodes and 3M Red Dot™ electrodes at the six precordial lead locations. We did not test the effect of stain on electrodes at V1 and V2 locations, because breathing movements do not put strain at those central locations.

	V1 (dB)	V2 (dB)	V3 (dB)	V4 (dB)	V5 (dB)	V6 (dB)
Our KT electrodes, unstrained	11.56	9.79	13.35	14.36	13.55	13.95
Our KT electrodes under 30% tensile strain	/	/	13.44	10.64	13.38	13.60
3M Red Dot™ electrodes, unstrained	7.31	8.20	9.50	10.43	11.62	12.16

Furthermore, the 3M Red Dot electrodes and our device are compared by measuring on the same subject simultaneously. The results are shown in Figure S5 and the two sets of signals are similar in amplitude, which further proves the reliability of the tape electrode. The 3M electrode and tape electrode were placed as close as possible; thus some part of the 3M electrode foam pad was underneath the tape electrode, which interfered with the tape electrodes from adhering to the body compared to when it was used alone. Nonetheless, the tape electrode signal-to-noise was still providing comparable results as the gold standard 3M electrodes.

It is noteworthy that the KT band offers advantages for addressing common issues that interfere with facilitating good contact between the body and the electrode surface. The issues are chest hairs in males or the curved surface around breast tissues in females, for which conventional gel electrodes are too small and do not have enough adhesive area to stably attach onto the non-flat surface. For females, this attachment problem often leads to improper placement of the V3 electrode being displaced to beneath the breast rather than on the correct position.[16] Yet, an ECG electrode should be placed within a 2 cm radius of the correct location, or else the reduced signal quality would affect the diagnostic accuracy.[17] For the KT patch here, its stretchability and large adhesive area provides extra support and grip to curved surfaces as shown in the data taken on a female subject. The electrodes are thin and conformal, promoting tight electrode-skin contact and ushering in correct placement.

The tape electrodes have been applied on a healthy human subject continuously for 48 hours. The subject conducted everyday tasks as normal and took showers with the electrodes covered with Tegaderm Film (3M). The result is shown in Figure S6. The V5 electrode signal right after placement has the same SNR, 13.62 dB after being used for 24 hours, and still retained 9.90 dB after 48 hours. The reference electrode, which was placed on the subject's sternum, did not show obvious crack or peeling on day 2 of use. The subject's sweat did not interact with the adhesive on the KT or alter the surface characteristics of the silver electrode. After 48 hours of use, the subject's skin did not have rash or signs of allergic reaction.
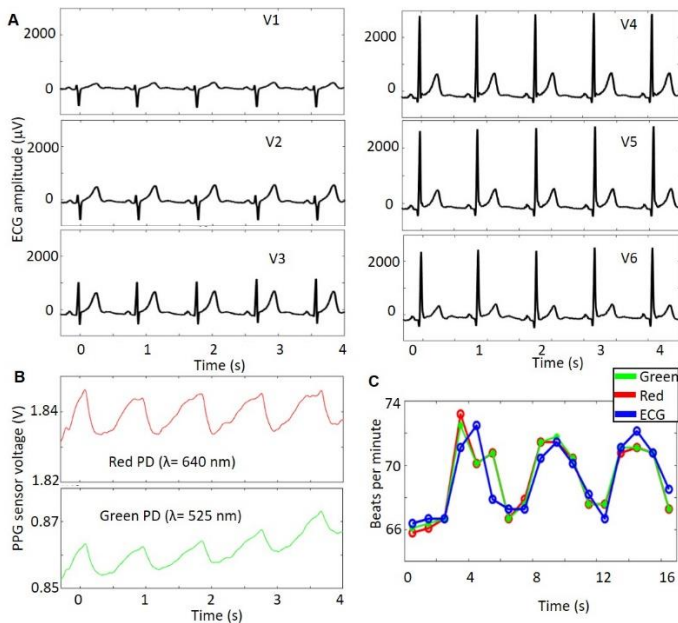

Figure 2. Simultaneous ECG and PPG measurements. Recordings have been captured for minutes, but here we zoom in only on few cycles to show the details. The subject was female. A) ECG signals from V1-V6 precordial leads. B) PPG signals taken by red and green photodiodes (PD). C) Instantaneous heart rate analysis, calculated by using data from the green or red photodiodes, or the V4 ECG lead indicated in blue.

B. Pulse oximetry in reflective mode

In addition to ECG electrodes, our KT band incorporates a pulse oximeter to track optical changes in tissue absorbance as a function of blood oxygenation. The light absorption of oxyhemoglobin (HbO_2) and de-oxyhemoglobin (Hb) are different at green and red wavelengths,[18,19] and by comparing the signal intensities at those two wavelengths, we can determine the blood oxygen saturation ratio [$SO_2 = HbO_2/(HbO_2+Hb)$]. An oxygen saturation level below 90% indicates hypoxia and demands immediate medical attention for the patient.

The PPG circuit in our design used a broad-spectrum white LED as the light source, and the light detectors were photodiodes with built-in bandpass filters transmitting wavelengths of 625—655 nm for the red photodiode and 510—540 nm for the green photodiode. Traditionally PPG circuit used infrared and red light emitting diodes and two corresponding photodiodes. Our circuit instead had one white LED and two photodiodes, which minimized the number of components and therefore reduced power consumption. Fewer components also required a smaller area for the device. Around the green wavelength, the difference between the molar extinction coefficient of oxygenated and deoxygenated hemoglobin is comparable to the difference at infrared wavelengths.[18] So the green and red combination could be more energy-efficient and compact while maintaining the same accuracy.

Here the PPG unit operated in reflective mode, in which the light arrived at the detectors by scattering through the tissue, in contrast to transmissive mode which measures changes through a thin body part such as in a fingertip or an earlobe. The reflective mode relaxed restrictions with regards to placement locations and allowed mounting of the PPG unit on the body core, specifically on top of the right subclavian artery in our demonstration. The PPG signal included a baseline absorption and a pulsatile feature.[18,20] The flow of oxygenated blood through the artery peaked and subsided with each cardiac cycle, leading to the cyclic signal in **Figure 2B**, which was essentially tracking heart beats.

The PPG and ECG data provided the basis to extract the metrics of heart rate and heart rate variability (HRV), defined as the ,time difference between each heartbeat. In context with additional symptoms, an abnormal HRV is an indicator for heart attack, sepsis,[21] and other pathological conditions. To use time-domain method to calculate the HRV, the time period *t* between each cardiac cycle was determined by processing the ECG or PPG signal through a peak picking algorithm to obtain the time between peaks, which are defined as normal-to-normal (NN) intervals. Then either the standard deviation or the root mean square of the time between these NN intervals are calculated, depending on which statistical measure is chosen to calculate HRV.[22] In this work, with our recordings around 1 minute long, they should yield one value for HRV. So

we use a parameter "beats per minute" as a demonstration for our device's robust ability to obtain HRV.

Each measured time period between NN intervals was converted to beats per minute by bpm= (60 s)/t; for example, when t= 0.91 s, then bpm = 66 for that instance. The ECG and PPG were taken simultaneously in Figure 2, and the HRVs extracted from the two independent measurements closely tracked each other as seen in **Figure 2C**. This high correlation[23] validated the PPG signal, that the reflective mode operation was properly monitoring cardiovascular changes. Then the data shown in **Figure 2C** is used in HRV calculation, which is the root mean square of successive NN intervals differences and should be 27±12ms.[22,24] The ECG signal yields a HRV of 57 ms, the red photodiode signal yields a HRV of 60 ms while green photodiode was HRV of 42 ms. The subject's regular HRV from the commercial Max-Health-Band is around 50 ms. This further shows our device has the ability to obtain HRV that is comparable to commercial counterparts.

The PPG unit was compared against a commercial fitness watch (Max-Health-Band, or hBand, by Maxim Integrated) worn on the volunteer's left wrist as recommended in the user manual. During measurements, the person walked slowly on a hard surface and kept limb movements to the minimum. A high-pass filter with a cutoff at 0.5 Hz was applied to the PPG signals in **Figure 3A** to remove the DC offset. Even after filtering, the signal from the wrist watch showed higher drift than the signals from the photodiodes in the PPG unit on the KT band. Motion artifacts were more severe in the extremities compared to the torso,[25] and the KT adhered to skin tightly, further reducing motion and ambient light interference. The calculation of beats per minute from the wristwatch signal was not accurate due to the amplitude fluctuations that sometimes baffled the peak-picking algorithm. The histograms of beats per minute in **Figure 3B** were consistent between the two photodiodes on the KT tape and indicated higher reliability in the analysis.
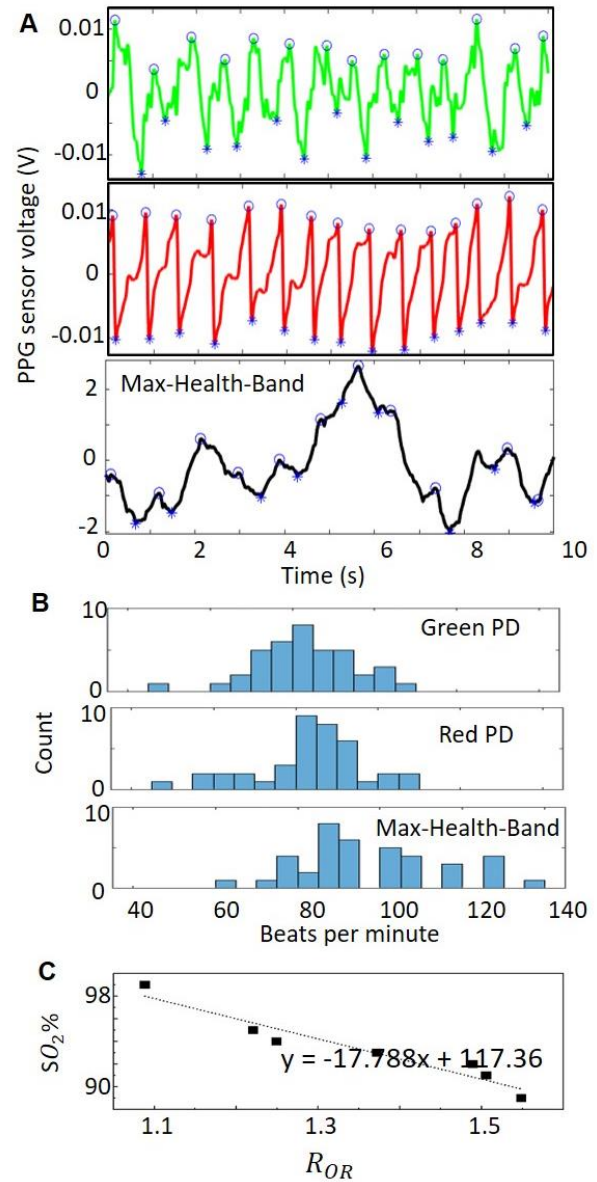

Figure 3. PPG signal stability and calibration. A) PPG signals from the green photodiode, the red photodiode, and the commercial health monitoring watch, Max-Health-Band. The open circles and star symbols represent peaks and troughs, respectively, in cardiac cycles. B) Histograms of heart rate calculated from the signals of photodiodes on the KT band (top and middle) and the wrist watch (bottom). C) Signal calibration according to Equation 1 and its linear fit versus blood oxygen saturation.

Through simultaneous measurements by red and green photodiodes of the scattered light from the subclavian artery, the ratio of the absorbances was calculated for correlation to blood oxygen saturation. The ratio of absorbances R at two different wavelengths λ were defined[26] as

$$R = \frac{AC_{\lambda,red}/DC_{\lambda,red}}{AC_{\lambda,green}/DC_{\lambda,green}} \quad \text{(Equation 1)},$$

where AC is the peak voltage of the pulsatile signal and DC is the stationary signal corresponding to the baseline trough
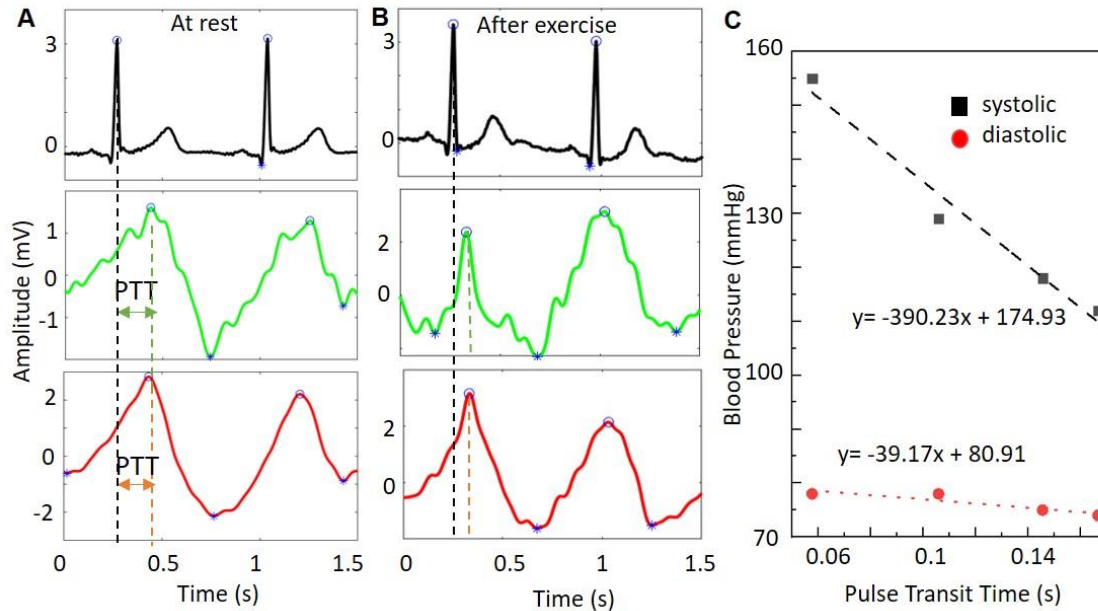
Figure 4. Combination of ECG and PPG to monitor blood pressure. The pulse transit time is determined from the time difference between the ECG R peak and the PPG systolic peaks. Measurements taken when the person was A) at rest and B) immediately after exercise. Top row: ECG at V4 location; middle row: PPG from the green photodiode. Bottom row: PPG from the red photodiode. C) Blood pressure calibration curves and linear fits.

voltage. The oxygen saturation level SO_2 has been shown to be correlated to R in previous works,[25,26] and the relationship of R and SO_2 was calibrated by using an altitude simulator (AltoLab BOOST) to vary the blood oxygen level in the volunteer, with the SO_2 being concurrently read out by a fingertip oximeter (Santamedical). The altitude simulator mixed exhaled air back into an air compartment and resulted in decreased oxygen content in the air for inhalation, thus leading to reduced SO_2 level in the person. In the calibration curve of **Figure 3C**, as the SO_2 level decreased from 99% to 89%, the measured R at the subclavian artery was shown to increase from 1.07 to 1.55. The data were fitted to obtain the fit equation in Figure 3C, which allows the extrapolation of SO_2 from R values. The extrapolation equation is not tested for generalization to account for body differences; for example, the scattering path through larger bodies would change the fit values. Nonetheless, by taking an initial SO_2 measurement and observing the trend of R values over time for an individual, the level of SO_2 can be monitored continuously by the PPG unit placed on the body core with less motion artifacts compared to fingertip oximeters.

C. Blood pressure inference

As the multimodal KT band captures ECG and PPG simultaneously, the relative shift between the two signals provides an important basis for inferring blood pressure. Monitoring blood pressure is vital because severe hypertension could indicate myocardial ischemia, neurologic syndromes, or acute heart failure.[27] The auscultative method to measure blood pressure involves an inflatable cuff that periodically pinches off blood flow and is uncomfortable for continuous monitoring.[28] The alternative cuff-less method[29] uses the principle that ECG electrical signals originate the pumping action of the heart, and

it takes time for the pulsatile blood flow to propagate to the location of the PPG unit over the subclavian artery. The time difference between the R peak in ECG and the systolic peak in PPG is defined as the pulse transit time (PTT).[30,31] With a higher blood pressure, the flow velocity increases, and therefore the PTT is decreased.

In **Figures 4A** and **4B**, the dashed lines denoted the PTT durations obtained by the peak-picking algorithm, and the measurements were recorded on a volunteer at rest and immediately after exercise, respectively. The PPT was reduced by exercise because the heart pumped harder during physical activities and resulted in higher pressure and faster blood flow than at rest. The PTTs determined by using green or red photodiode signals were the same, demonstrating reliability. In **Figure 4C**, the calibration data of PTT versus blood pressure were taken in the period when the volunteer was cooling down after exercising for 10 minutes. The person was wearing the KT band and a commercial blood pressure monitoring cuff (Omron BP250) on the left arm. During the cooling period, the systolic blood pressure changed from 155 to 112 mmHg, and the diastolic blood pressure changed from 78mmHg to 74mmHg, corresponding to the PTT increased from 0.05 s to 1.16 s. The data were fitted to linear equations as shown in Figure 4C for conversion of the measured PTT to systolic and diastolic blood pressures. Here the fit values were person-specific, as PTT would be affected by factors including wall thickness of blood vessels, density of the blood, etc. However, the trend in PTTs is useful for monitoring acute changes in a patient, such as to evaluate shock index (defined as heart rate/systolic blood pressure)[32] and potential malperfusion.[33]

This study is taken out healthy volunteers. For patients who are hemodynamically unstable, the blood pressure estimations may demonstrate greater variations. Thus monitoring patients under states of severe physiologic derangement may require more frequent sampling of beat-to-beat variability in emergency settings, which can be implemented in our system.

III. CONCLUSION

This work presents a multimodal ECG and PPG interface to improve the efficiency and accuracy of patient monitoring. The stretchable, integrated system minimizes the possibility of electrode misplacement and takes advantage of the KT textile substrate to quickly and securely attach sensors and reduce motion artifacts. The dry precordial electrodes provide the same signal quality as commercial gel electrodes without the risk of gel dehydration. The PPG signals are more stable from our KT band than from a commercial health monitoring watch because of better device placement. Moreover, the synergistic combination of ECG and PPG enables blood pressure monitoring through determination of PTT, which provides the benefit of eliminating bulky pneumatic cuff equipment. The KT band design can be further extended in the future to include a temperature sensor and strain sensors for respiratory cycles and complete the full suite of vital sign monitoring. The stretchable platform is user-friendly and low-cost for practical clinical implementations.

Appendix: Experiment Procedures
Two healthy volunteers, one male and the other female provided signed consent to participate in this study.

Fabrication process for the ECG interface

The kinesiology tape (Spidertech, Extra Wide Roll) is cut into a 20 cm by 12 cm band. The stencil was made by a stencil cutter (Silhouette, Cameo3) patterning mylar sheets with a thickness of 0.14 mm. The thermoplastic polyurethane base film (Intexar TE-11C) was cut to match the outline of the electrodes. The Ag/AgCl ink (Ercon E2414) was mixed with Ecoflex (Smooth-on, Ecoflex 00-50) at a weight ratio of 94:6.[9,34–36] The Ag/AgCl ink mixture was screen-printed[37,38] on the base film and cured at 100 °C for 10 mins. We printed onto the base film and did not directly print onto textiles, to avoid ink spreading on textiles that lowered printed line resolution and conductivity. The base film with printed electrodes was placed onto the KT band then heat-pressed at 130 °C for 1 min. A hole of 0.2 cm diameter was punched at the end of each interconnect. Then a conductive epoxy (Chemtronics, CW2460-ND) was applied around the hole. The components of a snap button, comprising of the stud (DOT® Medical Studs, 96-NS-90307-3U) and the post (Select Engineering, S-9001/335/0.075), were installed through the punched hole. For encapsulation, a thin layer of Ecoflex (Smooth-on, Ecoflex 00-50) was applied on top of snap button and the serpentine interconnects. The whole tape was cured at 100 °C for 10 min.

ECG recording

In this study, an OpenBCI Cyton board was used to collect ECG and PPG signals simultaneously. The sampling frequency was 250 Hz and set to an amplifier gain of 24. The ECG signals were processed with the following filters: 1) high-pass filter with a cutoff at 0.5 Hz 2) Butterworth band-stop filters at 60 Hz and 50 Hz, in which the bandwidth of the filters is 2Hz. The high-pass filter was used to remove the DC offset and drift. The band-stop filters were used to remove the powerline noise.

There are many methods to evaluate ECG signal quality, such as Karhunen-Loeve transform and signal quality indices.[39] However, given the trade-offs between complexity and prevalence in applications, we chose to evaluate ECG signals with the signal-to-noise (SNR) ratio. The SNRs reported in the literature[40] encompassed a wide range from -9.8 dB to 21.7 dB depending on varying definitions and different de-noising methods.[41,42] Our calculations here yielded values that fit within the typical range. We selected the same length period of noise and signal to calculate SNR, as shown in Figure S7.

Fabrication process for the pulse oximetry circuit

The kinesiology tape (Spidertech, Extra Wide Roll) was cut into a 7 cm by 9 cm rectangle. Copper tape (Bright Creations) was cut into the desired pattern by a stencil cutter (Cameo3). The green and red photodiodes were silicon PIN photodiode with an active area of 0.18 mm^2. They had a built-in bandpass filter of 625-655nm for the red photodiode and 510-540nm for the green photodiode (Advanced Photonix, 019-141-411-G, 019-141-411-R). The light source is a white LED (American Opto Plus LED, L196L-NWC). The resistors in series with the photodiodes were 2MΩ and the one in series with the LED was 100 Ω. The chosen components were small surface-mount packages. The components were soldered onto the copper tape on the textile substrate.

Pulse oximetry recording

The pulse oximetry circuit was placed on the volunteer's subclavian area such that both the green and red photodiodes were aligned with the subclavian artery. The circuit was powered by a USB Battery Pack (2200 mAh, 5 V 1A Output, Adafruit). The green and red photodiode outputs were read by the OpenBCI Cyton board. The input gain for the photodiode channels was set to x1. The photodiode signals were processed with a low-pass filter with a cutoff at 2 Hz to remove high-frequency noise.

ECG electrode characterization

Spectral noise measurements: The OpenBCI board (Cyton biosensing board Kit, OpenBCI) was used to record the noise spectra. Two electrodes were placed face-to-face. One electrode was connected to the positive pin of a channel, and the other electrode to the negative pin of the same channel. For the equipment noise, no device were connected, and the input pins were directly connected by a wire. For each recording, the voltage across the electrodes or wire was measured for 55 s. Three recordings were used to plot the noise spectra with error bars. The time-domain data was transformed into frequency-domain data by the Matlab periodogram function, there were no

filters applied to the signal. The peak at 60 Hz was due to the power-line noise.

A potentiostat (Bio-Logic SP-200) was used to record the electrodes' electrochemical impedance spectroscopy (EIS). The EIS was measured in a two-electrode configuration. During the test, the two were put face-to-face. The potentiostat supplied a sinusoidal signal with peak-to-peak amplitude of 10 mV and at 0 V dc bias.

PPG signal processing for HRV calculation

The ECG signal chosen to calculate HRV was taken at the V4 lead, because V4 showed the highest R-peak among the precordial leads. The max/min points in the PPG signal were found with Matlab. The functions were 'islocalmin' and 'islocalmax'. The local window to search for the max/min was adjusted according to the extracted heart rate to improve the processing results.

Supporting Information

Supporting Information is available from the journal website or from the author.

REFERENCES

(1) Zègre-Hemsey, J. K.; Garvey, J. L.; Carey, M. G. Cardiac Monitoring in the Emergency Department. *Critical Care Nursing Clinics of North America* **2016**, *28* (3), 331–345.

(2) Medani, S. A.; Hensey, M.; Caples, N.; Owens, P. Accuracy in Precordial ECG Lead Placement: Improving Performance through a Peer-Led Educational Intervention. *Journal of Electrocardiology* **2018**, *51* (1), 50–54.

(3) Kim, T.; Bao, C.; Chen, Z.; Kim, W. S. 3D Printed Leech-Inspired Origami Dry Electrodes for Electrophysiology Sensing Robots. *Npj Flexible Electronics* **2022**, *6* (5), 1–30.

(4) Khan, Y.; Ostfeld, A. E.; Lochner, C. M.; Pierre, A.; Arias, A. C. Monitoring of Vital Signs with Flexible and Wearable Medical Devices. *Advanced Materials* **2016**, *28* (22), 4373–4395.

(5) Chen, S.; Qi, J.; Fan, S.; Qiao, Z.; Yeo, J. C.; Lim, C. T. Flexible Wearable Sensors for Cardiovascular Health Monitoring. *Advanced Healthcare Materials* **2021**, *10* (17), 1–23.

(6) Vuorinen, T.; Noponen, K.; Jeyhani, V.; Aslam, M. A.; Junttila, M. J.; Tulppo, M. P.; Kaikkonen, K. S.; Huikuri, H. V.; Seppänen, T.; Mäntysalo, M.; Vehkaoja, A. Unobtrusive, Low-Cost Out-of-Hospital, and In-Hospital Measurement and Monitoring System. *Advanced Intelligent Systems* **2021**, *3* (3), 2000030.

(7) Roy, S. K.; Shah, S. U.; Villa-Lopez, E.; Murillo, M.; Arenas, N.; Oshima, K.; Chang, R. K.; Lauzon, M.; Guo, X.; Pillutla, P. Comparison of Electrocardiogram Quality and Clinical Interpretations Using Prepositioned ECG Electrodes and Conventional Individual Electrodes. *Journal of Electrocardiology* **2020**, *59*, 126–133.

(8) Wu, Y.; Mechael, S. S.; Lerma, C.; Carmichael, R. S.; Carmichael, T. B. Stretchable Ultrasheer Fabrics as Semitransparent Electrodes for Wearable Light-Emitting e-Textiles with Changeable Display Patterns. *Matter* **2020**, *2* (4), 882–895.

(9) Wang, K.; Parekh, U.; Pailla, T.; Garudadri, H.; Gilja, V.; Ng, T. N. Stretchable Dry Electrodes with Concentric Ring Geometry for Enhancing Spatial Resolution in Electrophysiology. *Advanced Healthcare Materials* **2017**, *6* (19), 1700552.

(10) Zhang, Y.; Xu, S.; Fu, H.; Lee, J.; Su, J.; Hwang, K. C.; Rogers, J. A.; Huang, Y. Buckling in Serpentine Microstructures and Applications in Elastomer-Supported Ultra-Stretchable Electronics with High Areal Coverage. *Soft Matter* **2013**, *9* (33), 8062–8070.

(11) Lyu, Q.; Gong, S.; Yin, J.; Dyson, J. M.; Cheng, W. Soft Wearable Healthcare Materials and Devices. *Advanced Healthcare Materials* **2021**, *10* (17), 1–34.

(12) Gruetzmann, A.; Hansen, S.; Müller, J. Novel Dry Electrodes for ECG Monitoring. *Physiological Measurement* **2007**, *28* (11), 1375–1390.

(13) Yamamoto, Y.; Yamamoto, D.; Takada, M.; Naito, H.; Arie, T.; Akita, S.; Takei, K. Efficient Skin Temperature Sensor and Stable Gel-Less Sticky ECG Sensor for a Wearable Flexible Healthcare Patch. *Advanced Healthcare Materials* **2017**, *6* (17), 1–7.

(14) Kisannagar, R. R.; Jha, P.; Navalkar, A.; Maji, S. K.; Gupta, D. Fabrication of Silver Nanowire/Polydimethylsiloxane Dry Electrodes by a Vacuum Filtration Method for Electrophysiological Signal Monitoring. *ACS Omega* **2020**, *5* (18), 10260–10265.

(15) Yoneyama, K.; Naka, M.; Harada, T.; Akashi, Y. Creating 12-Lead Electrocardiogram Waveforms Using a Three-Lead Bedside Monitor to Ensure Appropriate Monitoring. *Journal of Arrhythmia* **2020**, *36* (6), 1107–1108.

(16) Rautaharju, P. M.; Park, L.; Rautaharju, F. S.; Crow, R. A Standardized Procedure for Locating and Documenting ECG Chest Electrode Positions: Consideration of the Effect of Breast Tissue on ECG Amplitudes in Women. *Journal of Electrocardiology* **1998**, *31* (1), 17–29.

(17) Kania, M.; Rix, H.; Fereniec, M.; Zavala-Fernandez, H.; Janusek, D.; Mroczka, T.; Stix, G.; Maniewski, R. The Effect of Precordial Lead Displacement on ECG Morphology. *Medical and Biological Engineering and Computing* **2014**, *52* (2), 109–119.

(18) Lochner, C. M.; Khan, Y.; Pierre, A.; Arias, A. C. All-Organic Optoelectronic Sensor for Pulse Oximetry. *Nature Communications* **2014**, *5*, 5745.

(19) Meng, F.; Alayash, A. I. Determination of Extinction Coefficients of Human Hemoglobin in Various Redox States. *Analytical Biochemistry* **2017**, *521*, 11–19.

(20) Li, N.; Eedugurala, N.; Leem, D. S.; Azoulay, J. D.; Ng, T. N. Organic Upconversion Imager with Dual Electronic and Optical Readouts for Shortwave Infrared Light Detection. *Advanced Functional Materials* **2021**, *31*, 2100565.

(21) Barnaby, D.; Ferrick, K.; Kaplan, D. T.; Shah, S.; Bijur, P.; Gallagher, E. J. Heart Rate Variability in Emergency Department Patients with Sepsis. *Academic Emergency Medicine* **2002**, *9* (7), 661–670.

(22) Malik, M.; Camm, A. J.; Bigger, J. T.; Breithardt, G.; Cerutti, S.; Cohen, R. J.; Coumel, P.; Fallen, E. L.; Kennedy, H. L.; Kleiger, R. E.; Lombardi, F.; Malliani, A.; Moss, A. J.; Rottman, J. N.; Schmidt, G.; Schwartz, P. J.; Singer, D. H. Heart Rate Variability. Standards of Measurement, Physiological Interpretation, and Clinical Use. *European*

Heart Journal **1996**, *17* (3), 354–381.

(23) Lu, G.; Yang, F.; Taylor, J. A.; Stein, J. F. A Comparison of Photoplethysmography and ECG Recording to Analyse Heart Rate Variability in Healthy Subjects. *Journal of Medical Engineering and Technology* **2009**, *33* (8), 634–641.

(24) Shaffer, F.; Ginsberg, J. P. An Overview of Heart Rate Variability Metrics and Norms. *Frontiers in Public Health* **2017**, *5* (September), 1–17.

(25) Abdollahi, S.; Markvicka, E. J.; Majidi, C.; Feinberg, A. W. 3D Printing Silicone Elastomer for Patient-Specific Wearable Pulse Oximeter. *Advanced Healthcare Materials* **2020**, *9* (15), 1–9.

(26) Khan, Y.; Han, D.; Pierre, A.; Ting, J.; Wang, X.; Lochner, C. M.; Bovo, G.; Yaacobi-Gross, N.; Newsome, C.; Wilson, R.; Arias, A. C. A Flexible Organic Reflectance Oximeter Array. *Proceedings of the National Academy of Sciences* **2018**, *115* (47), E11015–E11024.

(27) Johnson, W.; Nguyen, M. Le; Patel, R. Hypertension Crisis in the Emergency Department. *Cardiology Clinics* **2012**, *30* (4), 533–543.

(28) Poon, C. C. Y.; Zhang, Y. T. Cuff-Less and Noninvasive Measurements of Arterial Blood Pressure by Pulse Transit Time. *Annual International Conference of the IEEE Engineering in Medicine and Biology - Proceedings* **2005**, *7 VOLS*, 5877–5880.

(29) Chen, W.; Kobayashi, T.; Ichikawa, S.; Takeuchi, Y.; Togawa, T. Continuous Estimation of Systolic Blood Pressure Using the Pulse Arrival Time and Intermittent Calibration. *Medical and Biological Engineering and Computing* **2000**, *38* (5), 569–574.

(30) McCarthy, B. M.; O'Flynn, B.; Mathewson, A. An Investigation of Pulse Transit Time as a Non-Invasive Blood Pressure Measurement Method. *Journal of Physics: Conference Series* **2011**, *307* (1).

(31) Luo, N.; Dai, W.; Li, C.; Zhou, Z.; Lu, L.; Poon, C. C. Y.; Chen, S. C.; Zhang, Y.; Zhao, N. Flexible Piezoresistive Sensor Patch Enabling Ultralow Power Cuffless Blood Pressure Measurement. *Advanced Functional Materials* **2016**, *26* (8), 1178–1187.

(32) Koch, E.; Lovett, S.; Nghiem, T.; Riggs, R. A.; Rech, M. A. Shock Index in the Emergency Department: Utility and Limitations. *Open Access Emergency Medicine* **2019**, *11*, 179–199.

(33) Liu, C.; Kim, J. T.; Kwak, S. S.; Hourlier-Fargette, A.; Avila, R.; Vogl, J.; Tzavelis, A.; Chung, H. U.; Lee, J. Y.; Kim, D. H.; Ryu, D.; Fields, K. B.; Ciatti, J. L.; Li, S.; Irie, M.; Bradley, A.; Shukla, A.; Chavez, J.; Dunne, E. C.; Kim, S. S.; Kim, J.; Park, J. Bin; Jo, H. H.; Kim, J.; Johnson, M. C.; Kwak, J. W.; Madhvapathy, S. R.; Xu, S.; Rand, C. M.; Marsillio, L. E.; Hong, S. J.; Huang, Y.; Weese-Mayer, D. E.; Rogers, J. A. Wireless, Skin-Interfaced Devices for Pediatric Critical Care: Application to Continuous, Noninvasive Blood Pressure Monitoring. *Advanced Healthcare Materials* **2021**, *10* (17), 1–16.

(34) Amit, M.; Chukoskie, L.; Skalsky, A. J.; Garudadri, H.; Ng, T. N. Flexible Pressure Sensors for Objective Assessment of Motor Disorders. *Advanced Functional Materials* **2019**, 1905241.

(35) Zhai, Y.; Wang, Z.; Kwon, K. S.; Cai, S.; Lipomi, D.; Ng, T. N. Printing Multi-Material Organic Haptic Actuators. *Advanced Materials* **2020**, 2002541.

(36) Amit, M.; Mishra, R. K.; Hoang, Q.; Galan, A. M.; Wang, J.; Ng, T. N. Point-of-Use Robotic Sensors for Simultaneous Pressure Detection and Chemical Analysis. *Materials Horizons* **2019**, *6*, 604–611.

(37) Bonnassieux, Y.; Brabec, C. J.; Cao, Y.; Carmichael, T. B.; Chabinyc, M. L.; Cheng, K.; Cho, G.; Chung, A.; Cobb, C. L.; Distler, A.; Egelhaaf, H.-J.; Grau, G.; Guo, X.; Haghiashtiani, G.; Huang, T.-C.; Hussain, M. M.; Iniguez, B.; Lee, T.; Li, L.; Ma, Y.; Ma, D.; McAlpine, M. C.; Ng, T. N.; Osterbacka, R.; Patel, S.; Peng, J.; Peng, H.; Rivnay, J.; Shao, L.; Steingart, D.; Street, R. A.; Subramanian, V.; Torsi, L.; Wu, Y. The 2021 Flexible and Printed Electronics Roadmap. *Flexible and Printed Electronics* **2021**, *6*, 023001.

(38) Kwon, K.; Ng, T. N. Improving Electroactive Polymer Actuator by Tuning Ionic Liquid Concentration. *Organic Electronics* **2014**, *15* (1), 294–298.

(39) Orphanidou, C.; Bonnici, T.; Charlton, P.; Clifton, D.; Vallance, D.; Tarassenko, L. Signal-Quality Indices for the Electrocardiogram and Photoplethysmogram: Derivation and Applications to Wireless Monitoring. *IEEE Journal of Biomedical and Health Informatics* **2015**, *19* (3), 832–838.

(40) Kaur, M.; Singh, B.; Seema. Comparison of Different Approaches for Removal of Baseline Wander from ECG Signal. *International Conference and Workshop on Emerging Trends in Technology 2011, ICWET 2011 - Conference Proceedings* **2011**, No. Icwet, 1290–1294.

(41) Del Río, B. A. S.; Lopetegi, T.; Romero, I. Assessment of Different Methods to Estimate Electrocardiogram Signal Quality. *Computing in Cardiology* **2011**, *38*, 609–612.

(42) Satija, U.; Ramkumar, B.; Sabarimalai Manikandan, M. A Review of Signal Processing Techniques for Electrocardiogram Signal Quality Assessment. *IEEE Reviews in Biomedical Engineering* **2018**, *11*, 36–52.